# Fast State-Space Harmonic-Distortion Estimation in Weakly Nonlinear $G_m-C$ Filters

Paul P. Sotiriadis, *Member, IEEE*, Abdullah Çelik, *Student Member, IEEE*, Dimitrios Loizos, *Student Member, IEEE*, and Zhaonian Zhang, *Student Member, IEEE*

***Abstract*—A fast, one-pass harmonic-distortion estimation algorithm for $G_m-C$ filters is introduced. It is derived using state-space modeling and can be applied directly to $G_m-C$ filters, of any order, with MOS transconductors exhibiting any type of weak nonlinearity. The algorithm is formed out of a small number of simple and explicit expressions involving the filter's structural matrices and the transconductors' nonlinearity. It can be easily implemented in MATLAB. For verification of the theoretical development, the algorithm was used to derive the harmonic distortion of a single-ended $G_m-C$ filter with weakly nonlinear transconductors designed on a 0.5-$\mu$m technology. The results of the algorithm and CADENCE simulation were found to be in good agreement.**

***Index Terms*—Author, please supply your own keywords or send a blank e-mail to keywords@ieee.org to receive a list of suggested keywords.**

## I. Introduction

During the past two decades, $G_m-C$ filter techniques have attracted a great deal of attention in the design of continuous-time filters. They have been favorable candidates in many high-frequency applications due to their tunability, low power, and wide bandwidth [1]–[12].

To achieve high-frequency performance, linearity is often sacrificed for faster and simpler transconductors that usually exhibit certain nonlinear behavior. This results in distortion at the filter's output.

When a sinusoidal signal of frequency $\omega$ is applied to the input of the filter, the output signal consists of not only the fundamental frequency component $\omega$, but also those at harmonics of the input frequency, i.e., 2 $\omega$, 3 $\omega$, and 4 $\omega, \ldots$. These terms form the *harmonic distortion*.

Harmonic distortion is a major issue in anti-aliasing filters preceding analog-to-digital converters (ADCs). Suppose, for example, that the input signal to an ADC is a sinusoidal at 400 kHz and the sampling frequency is 1.5 MHz. The third-order harmonic component at the output of the anti-aliasing filter will be at 1200 kHz and thus aliased at 300 kHz. This undesirable component at 300 kHz directly degrades the effective SNR of the analog-to-digital (A/D) conversion process by corrupting the useful signal.

Manuscript received August 9, 2006; revised September 11, 2006. This paper was recommended by Associate Editor T. B. Tarim.

P. P. Sotiriadis, D. Loizos, and Z. Zhang are with the Department of Electrical Engineering, The Johns Hopkins University, Baltimore, MD 21218 USA (e-mail: pps@jhu.edu).

A. Çelik is with **[AUTHOR: PLEASE PROVIDE A COMPLETE MAILING ADDRESS.—ED.]**MAXIM.

Digital Object Identifier 10.1109/TCSI.2006.887458

In addition, harmonic distortion partially determines the dynamic range of a filter [13]. Over the past two decades, significant effort has been made to optimize filters in terms of their dynamic range and power dissipation. Companding, scaling, and other techniques have been employed to improve the dynamic range and reduce nonlinearity [1], [14]–[18]. Accurate knowledge of the harmonic distortion of the filters is important for these efforts.

Techniques have been developed to calculate the harmonic distortion in filters and amplifiers [19]–[24]. The Volterra series approach is used in almost all of them [19]–[21] where the nonlinear system is decomposed into an infinite number of subsystems with polynomial nonlinearities and the harmonic components are evaluated separately for each subsystem.

Another approach was presented in [25], where partial transfer functions, from the input to internal nodes of the filter, were used to derive the output harmonic distortion.

This paper introduces a general, fast one-pass harmonic-distortion estimation algorithm that is based on state-space representation of the filter and can be applied directly to $G_m-C$ filters of *any order* and with MOS transconductors exhibiting any type of weak nonlinearity. Furthermore, the model of the transconductors used in the algorithm accounts for finite output impedance and offset. This allows the application of the algorithm to $G_m-C$ filters with simple transconductors used in certain cases under stringent speed and voltage supply requirements.

The results in this study extend the algorithm presented in [30] that applies only to fully balanced weakly nonlinear $G_m-C$ filters and does not account for finite output impedance of the transconductors nor their offset.

For verification of the theoretical development, a single-ended $G_m-C$ filter with weakly nonlinear MOS transconductors has been designed on a 0.5-$\mu$m technology. The harmonic distortion of the filter has been derived using CADENCE simulation and by applying the algorithm. The results were found to be in good agreement.

This paper is organized as follows. Section II introduces the model of trasconductors with weak, but otherwise arbitrary, nonlinearity and the state-space model of weakly nonlinear $G_m-C$ filters. Section III presents the structural decomposition of weakly nonlinear filters and their approximate state-space models. The derivation of the harmonic distortion, in the case of $G_m-C$ filters having transconductors with identical nonlinearity characteristics, performed done in Section IV. Section V presents simplified versions of the distortion estimation algorithm for $G_m-C$ filters with second- and third-order

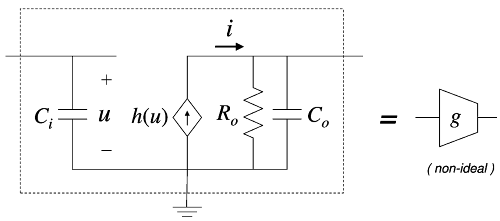


Fig. 1. Transconductor model.

nonlinearity. In Section VI, the algorithm is extended to $G_m{-}C$ filters with transconductors having more than one nonlinearity characteristic. CADENCE simulation results are presented in Section VII and compared with those derived using the proposed algorithm.

## II. Transconductor Model and Nonlinear $G_m{-}C$ Filter State-Space Representation

This section introduces the mathematical models, state-space formulation, notation, and assumptions used in this paper.

### A. Transconductors With Weak Nonlinearity and Offset

Although the analysis and results in this paper are valid for $G_m{-}C$ filters with single-ended or fully differential transconductors, single-ended notation is used for simplicity.

Fig. 1 shows the transconductor model used in this study. It includes finite input and output impedances and nonlinear gain.

The output impedance is modeled by $R_o$ in parallel with $C_o$. Since the output is connected to a node of the $G_m{-}C$ filter, $C_o$ can be considered as part of the node's capacitance. The same can be done for the input parasitic capacitance, $C_i$. Therefore, there is no need to include the parasitic capacitances explicitly in the mathematical expressions. Also, since $G_m{-}C$ filters are almost always implemented in CMOS technologies no input parasitic resistance is considered.

Function $h$ in Fig. 1 captures the input–output $I$–$V$ characteristic (when the output is grounded) of the transconductor. We assume that $h$ has a Taylor series expansion

$$i = h(u) = -i_{of} + gu + g_2u^2 + g_3u^3 + \cdots \tag{1}$$

where $i_{\rm of}$ is the output offset current, $g$ is the (linear) gain of the transconductor, and $g_2, g_3, \ldots,$ are the coefficients of the second-order and higher order nonlinear terms.

It is common in practice that the offset $i_{\rm of}$ and the nonlinear terms $g_2u^2, g_3u^3, \ldots,$ are proportional to the (linear) gain $g$, e.g., connecting two identical transconductors in parallel or doubling the widths of the output MOS transistors results in twice the gain $g$ and in twice the output offset current and the nonlinear terms (at least in MOS transonductors). Therefore, we can write

$$i = -gu_{\rm of} + gu + g\tilde{h}(u) \tag{2}$$

where $u_{\rm of} = i_{\rm of}/g$ and function $\tilde{h} = (g_2/g)u^2 + (g_3/g)u^3 + \ldots$. Similar reasoning leads to

$$R_o = 1/(\mu g) \tag{3}$$

for an appropriate dimensionless constant $\mu$.

The nonlinear term $g\tilde{h}(u)$ in (2) is by assumption (absolutely) small compared with the desirable term $gu$. From (1) and (2), we have

$$g\tilde{h}(u)/u = g_2u + g_3u^2 + \cdots$$

which depends strongly on $u$, and it can become absolutely greater than 1 for sufficiently large $u$. Therefore, the range of $u$ must be taken into account. Let $u_M$ be an estimate of the maximum absolute value of $u$ that is expected during the operation of the filter. Define

$$\delta \triangleq \max_{-u_M \le u \le u_M} \left| \frac{\tilde{h}(u)}{u} \right|. \tag{4}$$

Parameter $\delta$ captures the "smallness" of the nonlinear terms and, in most cases, knowledge of its exact value is not necessary. It can be set using an empirical estimation or a simulation result. Parameter $\delta$ has dimensions $V^{-1}$. Defining

$$f(u) = \tilde{h}(u)/\delta \tag{5}$$

we can write (1) as

$$i = -gu_{\rm of} + gu + \delta g f(u). \tag{6}$$

Note that $gf(u)$ can take values comparable with $gu$ and that $\delta$ is small by assumption. Equation (6) models the transconductors' behavior in the rest of the paper. Certain functions $f$ will be considered, e.g., in fully differential transconductors, it is $f(u) \approxeq u^3$.

Transconductance $g$, parameters $u_{\rm of}$ and $\delta$, as well as function $f$ can be derived by fitting a polynomial to the $I$–$V$ characteristic of the transconductor, as was done in Section VII. Analytical derivation of $g$ and $\delta$ and $f$ is also possible.

### B. State-Space Models of Nonlinear $G_m{-}C$ Filters

A linear $n$th-order $G_m{-}C$ filter (with ideal transconductors) can be treated as a single-input single-output (SISO) linear dynamical system with, say, input $u$, output $y$, and state vector $\mathbf{v} = (v_1, v_2, \ldots, v_n)^T$, where $v_i$ is the voltage of the $i$th capacitor, $i = 1, 2, \ldots, n$. In this case, the state-space equations of the filter are

$$\begin{aligned} \dot{\mathbf{v}} &= A\mathbf{v} + Bu \\ y &= L^T\mathbf{v} \end{aligned} \tag{7}$$

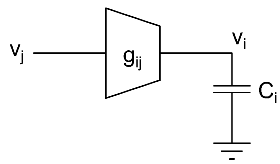


Fig. 2. Transconductor model.

where $A = [g_{i,j}/C_i]_{i,j=1}^n$ is the $n \times n$ system matrix and $B = [g_i^I/C_i]_{i=1}^n$ is the $n \times 1$ input vector. Here, $g_{i,j}$ is the gain of the transconductor with the input connected to node $j$ and the output connected to node $i$, as shown in Fig. 2. If such a transconductor does not exist, then we set $g_{i,j} = 0$. Similarly, $g_i^I$ is the gain of the transconductor from the input $u$ to the $i$th (node) capacitor.

Finally, $L^T$ is the $1 \times n$ output row vector. If the output is simply a state variable of the filter, as it is in many $G_m - C$ filters, then $L^T = [0, \ldots, 0, 1, 0, \ldots, 0]$. If the output is a current, then $L = [g_i^O]_{i=1}^n$, where $g_i^O$ is the gain of the transconductor from node $i$ to the output.

The transfer function of the filter is

$$H(s) = L^T(sI - A)^{-1}Bu.$$

Now, we derive the model of the weakly nonlinear filter based on the transconductor's model shown in Fig. 1 and the $I$–$V$ relation given by (6). It is assumed that the input and output parasitic capacitances of transconductors have been included into the filter's nodal capacitances $C_i$'s. It is

$$C_i \dot{v}_i = \sum_{j=1}^{n} \left( i_{i,j} - \frac{v_i}{(R_o)_{i,j}} \right) + i_i^I - \frac{v_i}{(R_o)_i^I} \tag{8}$$

where $i_{i,j}$ is the output current of the $(i,j)$ tranconductor (measured with grounded output) and $v_i/(R_o)_{i,j}$ is the part of this current consumed by $(R_o)_{i,j}$. Similarly, the (total) current provided to the $i$th node by the $i$th input transconductor is given by the sum of the last two terms.

Equations (3) and (6) are replaced in (8) to give

$$\begin{aligned} C_i \dot{v}_i = &\sum_{j=1}^{n} g_{i,j}(-u_{\rm of} + v_j + \delta f(v_j) - \mu v_i) \\ &+ g_i^I(-u_{\rm of} + u + \delta f(u) - \mu v_i). \end{aligned} \tag{9}$$

Some definitions are in order: $\mathbf{v} = (v_1, v_2, \ldots, v_n)^T$ is the state vector, $\mathbf{C} = \operatorname{diag}(C_1, C_2, \ldots, C_n)$ is the $n \times n$ diagonal capacitance matrix, $G = [g_{i,j}]_{i,j=1}^n$ is the transconductance matrix, $G^I = [g_i^I]_{i=1}^n$ is the $n \times 1$ input transconductance vector, $\mathbf{1} = [1, 1, \ldots, 1]^T$ is the $n \times 1$ all-ones vector, and $\mathbf{F}(\mathbf{v}) = [f(v_1), f(v_2), \ldots, f(v_n)]^T$ is a vector function.

Equation (9) is written in vector form as

$$\begin{aligned} \mathbf{C}\dot{\mathbf{v}} = &-u_{\rm of}\mathbf{G}\mathbf{1} + \mathbf{G}\mathbf{v} + \delta\mathbf{G}\mathbf{F}(\mathbf{v}) - \mu \operatorname{diag}(\mathbf{G}\mathbf{1})\mathbf{v} \\ &- u_{\rm of}\mathbf{G}^I + \mathbf{G}^I u + \delta\mathbf{G}^I f(u) \\ &- \mu \operatorname{diag}(\mathbf{G}^I)\mathbf{v}. \end{aligned} \tag{10}$$

Grouping of the terms in (10) gives

$$\begin{aligned} \mathbf{C}\dot{\mathbf{v}} = &-u_{\rm of}(\mathbf{G}\mathbf{1} + \mathbf{G}^I) \\ &+ (\mathbf{G} - \mu \operatorname{diag}(\mathbf{G}\mathbf{1} + \mathbf{G}^I))\mathbf{v} \\ &+ \delta\mathbf{G}\mathbf{F}(\mathbf{v}) + \mathbf{G}^I u + \delta\mathbf{G}^I f(u). \end{aligned} \tag{11}$$

Additional definitions are

$$\mathbf{M} = \mathbf{C}^{-1}\mathbf{G} \tag{12}$$
$$\mathbf{A} = \mathbf{C}^{-1}\mathbf{G} - \mu\mathbf{C}^{-1}\operatorname{diag}(\mathbf{G}\mathbf{1} + \mathbf{G}^I) \tag{13}$$
$$\mathbf{B} = \mathbf{C}^{-1}\mathbf{G}^I \tag{14}$$
$$\mathbf{z} = u_{\rm of}\mathbf{C}^{-1}(\mathbf{G}\mathbf{1} + \mathbf{G}^I). \tag{15}$$

Replacing (12)–(15) in (10), we obtain the system equation of the nonlinear $G_m - C$ filter

$$\dot{\mathbf{v}} = -\mathbf{z} + \mathbf{A}\mathbf{v} + \delta\mathbf{M}\mathbf{F}(\mathbf{v}) + \mathbf{B}u + \delta\mathbf{B}f(u).$$

The output $y$ of the filter can be either: 1) the voltage of a filter's node i.e., $y = \mathbf{e}_k^T\mathbf{v}$, where $\mathbf{e}_k^T = (0, \ldots, 0, 1, 0, \ldots, 0)$, with the 1 being in the $k$th entry, or 2) in current form which using (6) implies

$$\begin{aligned} y &= \sum_{i=1}^{n} \left(-u_{\rm of}g_i^O + g_i^O v_i + \delta g_i^O f(v_i)\right) \\ &= -y_{\rm of} + \mathbf{L}^T\mathbf{v} + \delta\mathbf{L}^T\mathbf{F}(\mathbf{v}) \end{aligned} \tag{16}$$

where $\mathbf{L} = [g_i^O]_{i=1}^n$ is the $n \times 1$ output vector and

$$y_{\rm of} = u_{\rm of} \sum_{i=1}^{n} g_i^O. \tag{17}$$

In (16), the parasitic output impedance of the output transconductors have been ignored, (assuming that the input impedance of the circuit following the filter is much smaller).

Summarizing the above, the mathematical model of the weakly nonlinear filter used in this paper is given by (the systems of)

$$\dot{\mathbf{v}} = -\mathbf{z} + \mathbf{A}\mathbf{v} + \delta\mathbf{M}\mathbf{F}(\mathbf{v}) + \mathbf{B}u + \delta\mathbf{B}f(u) \tag{18}$$
$$y = -y_{\rm of} + \mathbf{L}^T\mathbf{v} + \delta\mathbf{L}^T\mathbf{F}(\mathbf{v}). \tag{19}$$

Equations (18) and (19) should be compared with the system (7) of the linear filter (bold matrices are used for the nonlinear filter).

*1) Example: Modeling a Second-Order $G_m - C$ Filter:* The general second-order $G_m$-$C$ filter[1] is shown in Fig. 3. If the

[1]A transconductor from the input directly to the output can be added to account for high-pass filters. Following the previous models, this path is static, and estimating the distortion it introduces is straightforward.

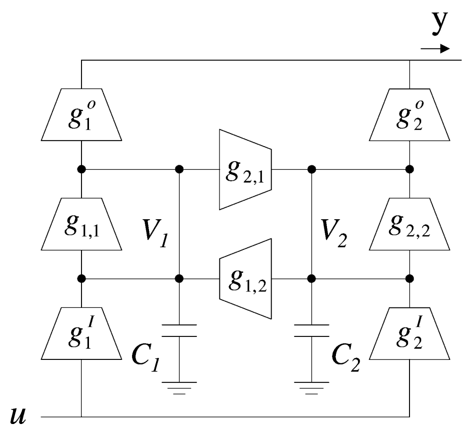


Fig. 3. General second-order $G_m-C$ filter.

transconductors are linear, then the filter is modeled by the set of equations (7), where

$$A = \begin{bmatrix} \frac{g_{1,1}}{C_1} & \frac{g_{1,2}}{C_1} \\ \frac{g_{2,1}}{C_2} & \frac{g_{2,2}}{C_2} \end{bmatrix}$$
$$B = \begin{bmatrix} \frac{g_1^I}{C_1} \\ \frac{g_2^I}{C_2} \end{bmatrix}$$
$$L = \begin{bmatrix} g_1^O \\ g_2^O \end{bmatrix}.$$

If the transconductors are nonlinear, then the filter is modeled by the set of (18) and (19), where

$$\mathbf{G} = \begin{bmatrix} g_{1,1} & g_{1,2} \\ g_{2,1} & g_{2,2} \end{bmatrix}$$
$$\mathbf{C}^{-1} = \begin{bmatrix} 1/C_1 & 0 \\ 0 & 1/C_2 \end{bmatrix}$$

and $\mathbf{G}^I = [g_1^I \; g_2^I]^T$. These imply structural matrices

$$\mathbf{z} = u_{\text{of}} \begin{bmatrix} \left(g_{1,1} + g_{1,2} + g_1^I\right)/C_1 \\ \left(g_{2,1} + g_{2,2} + g_2^I\right)/C_2 \end{bmatrix}$$
$$\mathbf{A} = \begin{bmatrix} \frac{g_{1,1} - \mu\left(g_{1,1} + g_{1,2} + g_1^I\right)}{C_1} & \frac{g_{1,2}}{C_1} \\ \frac{g_{2,1}}{C_2} & \frac{g_{2,2} - \mu\left(g_{2,1} + g_{2,2} + g_2^I\right)}{C_2} \end{bmatrix}$$
$$\mathbf{M} = \begin{bmatrix} \frac{g_{1,1}}{C_1} & \frac{g_{1,2}}{C_1} \\ \frac{g_{2,1}}{C_2} & \frac{g_{2,2}}{C_2} \end{bmatrix}$$
$$\mathbf{F}(\mathbf{v}) = \begin{bmatrix} f(v_1) \\ f(v_2) \end{bmatrix}$$
$$\mathbf{B} = \begin{bmatrix} \frac{g_1^I}{C_1} \\ \frac{g_2^I}{C_2} \end{bmatrix}$$
$$\mathbf{L} = \begin{bmatrix} g_1^O \\ g_2^O \end{bmatrix}$$
$$y_{\text{of}} = u_{\text{of}} \left(g_1^O + g_2^O\right).$$

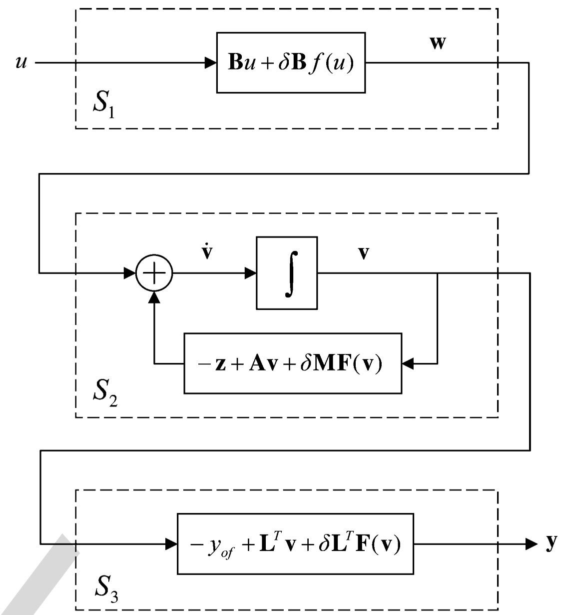


Fig. 4. $G_m-C$ filter viewed as a cascade of three stages.

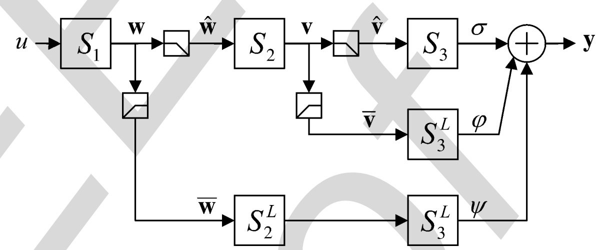


Fig. 5. Approximate system.

## III. Filter's Structural Decomposition

Throughout the paper, we assume that the (ideal) linear system in (7) is asymptotically stable and the input of the filter is $u = a\sin(\omega t)$.

The block diagram of the weakly nonlinear system modeled by (18) and (19) is shown in Fig. 4. The system can be viewed as a *cascade* of three stages, represented by operators $S_1, S_2$, and $S_3$, respectively, in the signal space[2] such that

$$\mathbf{w} = S_1(u)$$
$$\mathbf{v} = S_2(\mathbf{w})$$
$$y = S_3(\mathbf{v}).$$

The response of the whole system is given by the composite operation $y = (S_3 \circ S_2 \circ S_1)(u) = (S_3(S_2(S_1(u))))$.

It is assumed that the transconductors are weakly nonlinear; therefore, it is expected that the harmonic distortion introduced is relatively small, i.e., the amplitudes of the harmonics are much smaller than the amplitude of the fundamental in every node of the filter. This leads to the approximation of the filter shown in Fig. 5.

[2]We consider only the steady-state response of the stages in the case of a sinusoidal input $u$.

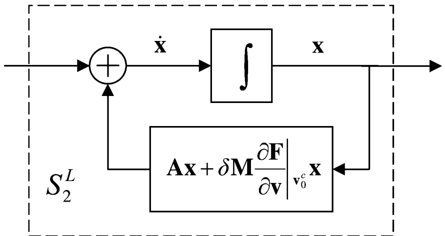


Fig. 6. Linearized second stage.

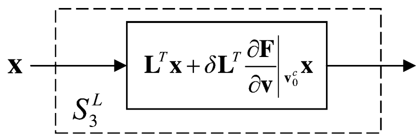


Fig. 7. Linearized third stage.

*Notation:* We use the decomposition of a signal $x$ in the form $x = \hat{x} + \bar{x}$, where $\hat{x}$ contains the dc and the fundamental frequency component, and $\bar{x} \triangleq x - \hat{x}$ contains the harmonic components.[3]

*Rationale:* The input $u = a\sin(\omega t)$ drives stage $S_1$ producing $\mathbf{w} = \hat{\mathbf{w}} + \bar{\mathbf{w}}$. The distortion component $\bar{\mathbf{w}}$ is expected to be very small compared with $\hat{\mathbf{w}}$, and therefore it does not impact the harmonic generation in stages $S_2$ and $S_3$ significantly. It approximately propagates to the output through the *linearized* versions of the stages $S_2^L$ and $S_3^L$. The distortion introduced by $S_2$ propagates similarly.

The linearized stages are shown in Figs. 6 and 7 where $\mathbf{v}_0^c$ is the dc component of $\mathbf{v}$. The offset of the transconductors must be taken into account in the linearization.

Finally, the output $y$ of the system in Fig. 5 is an approximation of the output signal in Fig. 4. It contains the approximate components of the fundamental and the harmonics generated by all three stages; $y = S_3(\hat{\mathbf{v}}) + S_3^L(\bar{\mathbf{v}}) + \left(S_3^L \circ S_2^L\right)(\bar{\mathbf{w}})$.

*Remark:* Variables $\mathbf{w}, \mathbf{v}$ and $y$ in Fig. 5 are approximations of $\mathbf{w}, \mathbf{v}$ and $y$ in Fig. 4. The use of the same symbols should not cause any confusion since from here on we consider only the approximate system in Fig. 5.

## IV. Harmonic-Distortion Estimation

Since the input is $u = a\sin(\omega t)$ and the (ideal) linear filter is assumed to be asymptotically stable, all signals in the filter will be periodic[4] of frequency $\omega$ and period $T = 2\pi/\omega$ [26]. Therefore, Fourier series representation can be used.

*Definition 4.1:* (Notation) For any vector or scalar signal $x$ in the filter, we write

$$x_k^c = \frac{2}{T}\int_0^T x(t)\cos(k\omega t)\,dt \tag{20}$$

$$x_k^s = \frac{2}{T}\int_0^T x(t)\sin(k\omega t)\,dt \tag{21}$$

for $k = 0, 1, 2, \ldots$. Therefore, the Fourier expansion of $x$ is $x(t) = x_0^c + \sum_{k=1}^{\infty}(x_k^c\cos(k\omega t) + x_k^s\sin(k\omega t))$ □

*Definition 4.2:* (Notation) For function $f$, defined by (5), and for every real numbers $\alpha, \beta$, and $\gamma$, we define

$$\begin{aligned} f_k^c(\alpha,\beta,\gamma) =& \frac{2}{T}\int_0^T f(\alpha+\beta\cos(\omega t)+\gamma\sin(\omega t)) \\ & \times \cos(k\omega t)\,dt \\ f_k^s(\alpha,\beta,\gamma) =& \frac{2}{T}\int_0^T f(\alpha+\beta\cos(\omega t)+\gamma\sin(\omega t)) \\ & \times \sin(k\omega t)\,dt \end{aligned}$$

for $k = 0, 1, 2, \ldots$. Therefore, we can write

$$\begin{aligned} f(\alpha+\beta\cos(\omega t)+\gamma\sin(\omega t)) =& f_0^c(\alpha,\beta,\gamma) \\ & + \sum_{k=1}^{\infty}\left(f_k^c(\alpha,\beta,\gamma)\cos(k\omega t)\right. \\ & \left. + f_k^s(\alpha,\beta,\gamma)\sin(k\omega t)\right). \end{aligned}$$

Similar notation is used for vector value function $\mathbf{F}$. □

The derivation of the harmonic distortion is done in steps using the approximate system in Fig. 5. First, we derive $\hat{\mathbf{w}}$ and $\bar{\mathbf{w}}$, then $\hat{\mathbf{v}}$ and $\bar{\mathbf{v}}$, and finally $y$.

### A. Derivation of $\hat{\mathbf{w}}$ and $\bar{\mathbf{w}}$

The input stage in Fig. 4 implies $\mathbf{w} = a\mathbf{B}\sin(\omega t) + \delta\mathbf{B}f(a\sin(\omega t))$, and thus $\hat{\mathbf{w}}$ can be approximated by

$$\hat{\mathbf{w}} \approxeq \mathbf{w}_1^s\sin(\omega t) \tag{22}$$

where $\mathbf{w}_1^s \approxeq a\mathbf{B}$, since $\mathbf{w}_0^c$ and $\mathbf{w}_1^c$ result only from the weak nonlinearity and are small and proportional to $\delta$. Note that the offsets of the input transconductors are taken into account in $\mathbf{z}$. For $\bar{\mathbf{w}}$, we have that

$$\bar{\mathbf{w}} = \sum_{k=2}^{\infty}\left(\mathbf{w}_k^c\cos(k\omega t) + \mathbf{w}_k^s\sin(k\omega t)\right) \tag{23}$$

where $\mathbf{w}_k^c = \delta\mathbf{B}f_k^c(0,0,a)$ and $\mathbf{w}_k^s = \delta\mathbf{B}f_k^s(0,0,a)$.

### B. Derivation of $\hat{\mathbf{v}}$ and $\bar{\mathbf{v}}$

The derivation of $\mathbf{v}$ is more tricky because it involves the solution of the nonlinear dynamical system

$$\dot{\mathbf{v}} = -\mathbf{z} + \mathbf{A}\mathbf{v} + \delta\mathbf{M}\mathbf{F}(\mathbf{v}) + \hat{\mathbf{w}} \tag{24}$$

(see Figs. 4 and 5). To this end, we employ regular perturbation theory [27]–[29] to derive an approximate solution.

The solution is expressed as a power series of $\delta$, i.e., $\mathbf{v} = \boldsymbol{\eta} + \delta\boldsymbol{\theta} + \delta^2\boldsymbol{\lambda} + \delta^3\boldsymbol{\xi}\ldots$, it is substituted into (24) and then the coefficients of the powers of $\delta$ at the left-hand and right-hand

[3]The low-pass and high-pass filters following stages $S_1$ and $S_2$ in Fig. 5 indicate this decomposition graphically.

[4]Some more technicalities are involved here.

sides of the equation are balanced. This results in an infinite set of systems of differential equations

$$\dot{\boldsymbol{\eta}} = -\mathbf{z} + \mathbf{A}\boldsymbol{\eta} + \hat{\mathbf{w}} \tag{25}$$
$$\dot{\boldsymbol{\theta}} = \mathbf{A}\boldsymbol{\theta} + \mathbf{M}\mathbf{F}(\boldsymbol{\eta}) \tag{26}$$
$$\dot{\boldsymbol{\lambda}} = \mathbf{A}\boldsymbol{\lambda} + \mathbf{M}\left.\frac{\partial \mathbf{F}}{\partial \mathbf{v}}\right|_{\eta} \boldsymbol{\theta} \tag{27}$$
$$\vdots$$

In principle, for sufficiently small $\delta$ and well-behaving $\mathbf{F}$, this set of equations can be solved providing the exact solution. In practice, the solution of the first two equations can provide an accurate result for small perturbations, $\delta\mathbf{MF}(\mathbf{v})$, [27]–[31].

From the result in Appendix I, (22), and (25), we have that

$$\boldsymbol{\eta} = \boldsymbol{\eta}_0^c + \boldsymbol{\eta}_1^c \cos(\omega t) + \boldsymbol{\eta}_1^s \sin(\omega t) \tag{28}$$

where $\boldsymbol{\eta}_0^c = \mathbf{A}^{-1}\mathbf{z}, \boldsymbol{\eta}_1^c = -(\omega^2\mathbf{I} + \mathbf{A}^2)^{-1}\omega\mathbf{w}_1^s$ and $\boldsymbol{\eta}_1^s = -(\omega^2\mathbf{I} + \mathbf{A}^2)^{-1}\mathbf{A}\mathbf{w}_1^s$. The solution of (26) is

$$\boldsymbol{\theta} = \boldsymbol{\theta}_0^c + \sum_{k=1}^{\infty} \left(\boldsymbol{\theta}_k^c \cos(k\omega t) + \boldsymbol{\theta}_k^s \sin(k\omega t)\right) \tag{29}$$

where

$$\boldsymbol{\theta}_0^c = -\mathbf{A}^{-1}\mathbf{M}\mathbf{F}_0^c\left(\boldsymbol{\eta}_0^c, \boldsymbol{\eta}_1^c, \boldsymbol{\eta}_1^s\right), \tag{30}$$
$$\begin{aligned}\boldsymbol{\theta}_k^c = &-\left(k^2\omega^2\mathbf{I} + \mathbf{A}^2\right)^{-1}\mathbf{A}\mathbf{M}\mathbf{F}_k^c\left(\boldsymbol{\eta}_0^c, \boldsymbol{\eta}_1^c, \boldsymbol{\eta}_1^s\right)\\ &-\left(k^2\omega^2\mathbf{I} + \mathbf{A}^2\right)^{-1}k\omega\mathbf{M}\mathbf{F}_k^s\left(\boldsymbol{\eta}_0^c, \boldsymbol{\eta}_1^c, \boldsymbol{\eta}_1^s\right)\end{aligned} \tag{31}$$
and
$$\begin{aligned}\boldsymbol{\theta}_k^s = &\left(k^2\omega^2\mathbf{I} + \mathbf{A}^2\right)^{-1}k\omega\mathbf{M}\mathbf{F}_k^c\left(\boldsymbol{\eta}_0^c, \boldsymbol{\eta}_1^c, \boldsymbol{\eta}_1^s\right)\\ &-\left(k^2\omega^2\mathbf{I} + \mathbf{A}^2\right)^{-1}\mathbf{A}\mathbf{M}\mathbf{F}_k^s\left(\boldsymbol{\eta}_0^c, \boldsymbol{\eta}_1^c, \boldsymbol{\eta}_1^s\right)\end{aligned} \tag{32}$$

for $k = 1, 2, 3, \ldots$

Combining (29) and (30) and using the approximation $\mathbf{v} \approxeq \boldsymbol{\eta} + \delta\boldsymbol{\theta}$, we conclude that

$$\hat{\mathbf{v}} \approxeq \boldsymbol{\eta}_0^c + \boldsymbol{\eta}_1^c \cos(\omega t) + \boldsymbol{\eta}_1^s \sin(\omega t) \tag{33}$$
and
$$\bar{\mathbf{v}} \approxeq \delta \sum_{k=2}^{\infty} \left(\boldsymbol{\theta}_k^c \cos(k\omega t) + \boldsymbol{\theta}_k^s \sin(k\omega t)\right). \tag{34}$$

### C. Derivation of $y$

First, we derive the distortion components of $y$. From Fig. 5, it is $\sigma = S_3(\hat{\mathbf{v}})$ which, along with (33), gives

$$\begin{aligned}\bar{\sigma} = &\delta\mathbf{L}^T \sum_{k=2}^{\infty} \left(\mathbf{F}_k^c(\boldsymbol{\eta}_0^c, \boldsymbol{\eta}_1^c, \boldsymbol{\eta}_1^s)\cos(k\omega t)\right.\\ &\left.+ \mathbf{F}_k^s(\boldsymbol{\eta}_0^c, \boldsymbol{\eta}_1^c, \boldsymbol{\eta}_1^s)\sin(k\omega t)\right).\end{aligned}$$

Operator $S_3^L$ in Fig. 7 can be approximated by $\mathbf{L}^T\mathbf{x}$. Since $\varphi = S_3^L(\bar{\mathbf{v}})$ in Fig. 5, using (34), we get

$$\bar{\varphi} \approxeq \delta\mathbf{L}^T \sum_{k=2}^{\infty} \left(\boldsymbol{\theta}_k^c \cos(k\omega t) + \boldsymbol{\theta}_k^s \sin(k\omega t)\right).$$

We also define $\psi = (S_3^L \circ S_2^L)(\bar{\mathbf{w}})$. Operator $S_3^L \circ S_2^L$ is linear and $\psi$ is derived using the result in Appendix I. Again, we use the approximation $S_3^L(\mathbf{x}) \approxeq \mathbf{L}^T\mathbf{x}$ as well as $\mathbf{A}\mathbf{x} + \delta\mathbf{M}(\partial\mathbf{F}/\partial\mathbf{v})|_{\mathbf{v}_0^c}\mathbf{x} \approxeq \mathbf{A}\mathbf{x}$. These lead to

$$\begin{aligned}\bar{\psi} \approxeq &-\mathbf{L}^T \sum_{k=2}^{\infty} (k^2\omega^2\mathbf{I} + A^2)^{-1}(\mathbf{A}\mathbf{w}_k^c + k\omega\mathbf{w}_k^s)\cos(k\omega t)\\ &+\mathbf{L}^T \sum_{k=2}^{\infty} (k^2\omega^2\mathbf{I} + A^2)^{-1}(k\omega\mathbf{w}_k^c - \mathbf{A}\mathbf{w}_k^s)\sin(k\omega t).\end{aligned}$$

The harmonic-distortion components of $y$ are given by the sum $\bar{\sigma} + \bar{\varphi} + \bar{\psi}$. Therefore

$$\bar{y} \approxeq \sum_{k=2}^{\infty} \left(y_k^c \cos(k\omega t) + y_k^s \sin(k\omega t)\right) \tag{35}$$

where

$$\begin{aligned}y_k^c \approxeq &\delta\mathbf{L}^T\mathbf{F}_k^c(\boldsymbol{\eta}_0^c + \delta\boldsymbol{\theta}_0^c, \boldsymbol{\eta}_1^c, \boldsymbol{\eta}_1^s) + \delta\mathbf{L}^T\boldsymbol{\theta}_k^c\\ &-\mathbf{L}^T(k^2\omega^2\mathbf{I} + A^2)^{-1}\left(\mathbf{A}\mathbf{w}_k^c + k\omega\mathbf{w}_k^s\right)\end{aligned} \tag{36}$$

and

$$\begin{aligned}y_k^s \approxeq &\delta\mathbf{L}^T\mathbf{F}_k^s\left(\boldsymbol{\eta}_0^c + \delta\boldsymbol{\theta}_0^c, \boldsymbol{\eta}_1^c, \boldsymbol{\eta}_1^s\right) + \delta\mathbf{L}^T\boldsymbol{\theta}_k^s\\ &+\mathbf{L}^T(k^2\omega^2\mathbf{I} + A^2)^{-1}\left(k\omega\mathbf{w}_k^c - \mathbf{A}\mathbf{w}_k^s\right).\end{aligned} \tag{37}$$

The fundamental frequency components of $y$ are derived by approximating the weakly nonlinear filter with the (ideal) linear one. The dc component is not required here. We have

$$\hat{y} \approxeq y_0^c + y_1^c \cos(\omega t) + y_1^s \sin(\omega t) \tag{38}$$

where

$$y_1^c \approxeq -\mathbf{L}^T(\omega^2\mathbf{I} + A^2)^{-1}\omega\mathbf{B}a \tag{39}$$
$$y_1^s \approxeq -\mathbf{L}^T(\omega^2\mathbf{I} + A^2)^{-1}\mathbf{A}\mathbf{B}a. \tag{40}$$

### D. Harmonic-Distortion Algorithm

The harmonic-distortion algorithm is summarized below. The vectors and matrices $\mathbf{A}, \mathbf{B}, \mathbf{L}, \mathbf{z}, \mathbf{M}$ as well as parameters $a$ and $\delta$, and functions $f, \mathbf{F}, f_k^c, f_k^s, \mathbf{F}_k^c$, and $\mathbf{F}_k^s$, are defined in Sections II–IV.

Index $k$ below ranges from 2 up to the highest order harmonic that is taken into account. The auxiliary variables $\mathbf{H}_k, R_k^c, R_k^s, Q_k^c$, and $Q_k^s$ are introduced to simplify notation. DC terms proportional to $\delta$ have been dropped for simplicity;

this should not impact the accuracy of the results as long as function $f$ is sufficiently smooth:

$$\begin{aligned}
\boldsymbol{\eta}_0^c &= \mathbf{A}^{-1}\mathbf{z} && (41)\\
\boldsymbol{\eta}_1^c &= -a\omega(\omega^2\mathbf{I}+\mathbf{A}^2)^{-1}\mathbf{B} && (42)\\
\boldsymbol{\eta}_1^s &= -a\mathbf{A}(\omega^2\mathbf{I}+\mathbf{A}^2)^{-1}\mathbf{B} && (43)\\
\mathbf{H}_k &\triangleq -(k^2\omega^2\mathbf{I}+\mathbf{A}^2)^{-1} && (44)\\
R_k^c &\triangleq \mathbf{F}_k^c(\boldsymbol{\eta}_0^c,\boldsymbol{\eta}_1^c,\boldsymbol{\eta}_1^s) && (45)\\
R_k^s &\triangleq \mathbf{F}_k^s(\boldsymbol{\eta}_0^c,\boldsymbol{\eta}_1^c,\boldsymbol{\eta}_1^s) && (46)\\
Q_k^c &= \mathbf{B}f_k^c(0,0,a) && (47)\\
Q_k^s &= \mathbf{B}f_k^s(0,0,a) && (48)\\
\boldsymbol{\theta}_k^c &= \mathbf{H}_k\left(\mathbf{A}\mathbf{M}R_k^c + k\omega\mathbf{M}R_k^s\right) &&\\
\boldsymbol{\theta}_k^s &= \mathbf{H}_k\left(-k\omega\mathbf{M}R_k^c + \mathbf{A}\mathbf{M}R_k^s\right) && (49)\\
y_1^c &\approxeq -\mathbf{L}^T\boldsymbol{\eta}_1^c && (50)\\
y_1^s &\approxeq -\mathbf{L}^T\boldsymbol{\eta}_1^s && (51)\\
y_k^c &\approxeq \delta\mathbf{L}^T\mathbf{H}_k\left(\mathbf{A}Q_k^c + k\omega Q_k^s\right) : \text{input} &&\\
&\quad + \delta\mathbf{L}^T\boldsymbol{\theta}_k^c : \text{core} && (52)\\
&\quad + \delta\mathbf{L}^T R_k^c : \text{output} &&\\
y_k^s &\approxeq \delta\mathbf{L}^T\mathbf{H}_k\left(-k\omega Q_k^c + \mathbf{A}Q_k^s\right) : \text{input} &&\\
&\quad + \delta\mathbf{L}^T\boldsymbol{\theta}_k^s : \text{core} && (53)\\
&\quad + \delta\mathbf{L}^T R_k^s : \text{output} &&\\
\bar{y} &\approxeq \sum_{k=2}^{\infty}\left(y_k^c\cos(k\omega t) + y_k^s\sin(k\omega t)\right) && (54)\\
\text{THD} &\approxeq \sqrt{\frac{\sum_{k=2}^{\infty}\left((y_k^c)^2+(y_k^s)^2\right)}{(y_1^c)^2+(y_1^s)^2}}. && (55)
\end{aligned}$$

*Remark:* The three terms of $y_k^c$ and $y_k^s$ correspond to distortion components introduced by the *input*, *core*, and *output* stages of the filter, respectively. If any of these stages is linear, or it is missing, then the corresponding terms should be removed. The THD is proportional to the "nonlinearity" parameter $\delta$.

## V. Two Special Cases

Transconductors with large output impedance, in most cases due to cascode output stages, and weak nonlinearity are frequently used in filter designs. These assumptions lead to the following two special cases of harmonic-distortion estimation.

### *A. Transconductors With Second- and Third-Order Nonlinearity, Zero Offset, and Infinite Output Impedance*

In many $G_m-C$ filters, the output impedance of the transconductors is large and does not influence the frequency behavior significantly. In this case, experience indicates that the harmonic-distortion behavior is not affected significantly either. Moreover, in most cases, the even and odd weakly nonlinear behaviors of the transconductors can be captured by the second and third nonlinear terms, respectively (i.e., the lowest even/odd nonlinear terms).

The above factors motivate the study of the general algorithm for the special case where $R_o = \infty$ and (1) is of the form $i = gu + g_2u^2 + g_3u^3$. Following (2), we have $\tilde{h}(u) = (g_2/g)u^2 + (g_3/g)u^3$ and, from (4), we get

$$\delta = \left|\frac{g_2}{g}\right| u_M + \left|\frac{g_3}{g}\right| u_M^2 \qquad (56)$$

where $u_M$ is the absolutely maximum value of $u$ (see the discussion in Section II-A). Function $f$ is

$$f(u) = \frac{\tilde{h}(u)}{\delta} = p_2u^2 + p_3u^3 \qquad (57)$$

where $p_2 = g_2/(\delta g)$ and $p_3 = g_3/(\delta g)$.

Since it is assumed that the transconductors have no offset, it must be $\mathbf{z} = 0$, and thus, from (41), we have $\boldsymbol{\eta}_0^c = 0$. Therefore, in the derivation of functions $f_k^c, f_k^s, \mathbf{F}_k^c$, and $\mathbf{F}_k^s$ in Definition 4.2, it is $\alpha = 0$. We have

$$\begin{aligned}
f_2^c(0,\beta,\gamma) &= -\frac{1}{2}p_2\gamma^2 + \frac{1}{2}p_2\beta^2\\
f_2^s(0,\beta,\gamma) &= p_2\beta\gamma\\
f_3^c(0,\beta,\gamma) &= \frac{1}{4}p_3\beta(-3\gamma^2+\beta^2)\\
f_3^s(0,\beta,\gamma) &= \frac{1}{4}p_3\gamma(3\beta^2-\gamma^2)\\
f_k^c(0,\beta,\gamma) &\equiv f_k^s(0,\beta,\gamma) \equiv 0, \qquad \text{for all } k \geq 4.
\end{aligned}$$

Moreover, $R_o = \infty$ implies that $\mathbf{A} = \mathbf{M}$ and so

$$\begin{aligned}
\boldsymbol{\eta}_1^c &= -a\omega(\omega^2\mathbf{I}+\mathbf{M}^2)^{-1}\mathbf{B}\\
\boldsymbol{\eta}_1^s &= -a\mathbf{M}(\omega^2\mathbf{I}+\mathbf{M}^2)^{-1}\mathbf{B}\\
\mathbf{H}_k &= -(k^2\omega^2\mathbf{I}+\mathbf{M}^2)^{-1}.
\end{aligned}$$

The above imply that

$$\begin{aligned}
R_2^c &= -\frac{1}{2}p_2(\boldsymbol{\eta}_1^s)^{\bullet 2} + \frac{1}{2}p_2(\boldsymbol{\eta}_1^c)^{\bullet 2}\\
R_2^s &= p_2\boldsymbol{\eta}_1^c \bullet \boldsymbol{\eta}_1^s\\
R_3^c &= \frac{1}{4}p_3\boldsymbol{\eta}_1^c \bullet \left(-3(\boldsymbol{\eta}_1^s)^{\bullet 2} + (\boldsymbol{\eta}_1^c)^{\bullet 2}\right)\\
R_3^s &= \frac{1}{4}p_3\boldsymbol{\eta}_1^s \bullet \left(3(\boldsymbol{\eta}_1^c)^{\bullet 2} - (\boldsymbol{\eta}_1^s)^{\bullet 2}\right)\\
R_k^c &= R_k^s = 0, \qquad \text{for all } k \geq 4
\end{aligned}$$

where "$\bullet$" is the Hadamard (entry-wise) product, and

$$\begin{aligned}
Q_2^c &= -\frac{1}{2}p_2a^2\mathbf{B}\\
Q_3^s &= -\frac{1}{4}p_3a^3\mathbf{B}\\
Q_2^s &= Q_3^c\\
&= Q_k^c\\
&= Q_k^s\\
&= 0, \qquad \text{for } k \geq 4.
\end{aligned}$$

Since $R_k^c, R_k^s, Q_k^c$, and $Q_k^s$ are zero for $k \geq 4$, the algorithm provides only the second and third harmonics; therefore, all expressions depending on $k$ must be evaluated for $k = 2, 3$ only.

Using $\mathbf{A} = \mathbf{M}$ again, we get

$$\boldsymbol{\theta}_k^c = \mathbf{H}_k \left(\mathbf{M}^2 R_k^c + k\omega \mathbf{M} R_k^s\right)$$
$$\boldsymbol{\theta}_k^s = \mathbf{H}_k \left(-k\omega \mathbf{M} R_k^c + \mathbf{M}^2 R_k^s\right)$$

and

$$y_1^c \approxeq -\mathbf{L}^T(\omega^2\mathbf{I} + \mathbf{M}^2)^{-1}\omega \mathbf{B} a$$
$$y_1^s \approxeq -\mathbf{L}^T(\omega^2\mathbf{I} + \mathbf{M}^2)^{-1}\mathbf{M}\mathbf{B} a.$$

Finally, the amplitudes of the harmonic components are

$$\begin{aligned} y_k^c \approxeq\, & \delta \mathbf{L}^T \mathbf{H}_k \left(\mathbf{M} Q_k^c + k\omega Q_k^s\right) : \text{input} \\ & + \delta \mathbf{L}^T \boldsymbol{\theta}_k^c : \text{core} \\ & + \delta \mathbf{L}^T R_k^c : \text{output} \\ y_k^s \approxeq\, & \delta \mathbf{L}^T \mathbf{H}_k \left(-k\omega Q_k^c + \mathbf{M} Q_k^s\right) : \text{input} \\ & + \delta \mathbf{L}^T \boldsymbol{\theta}_k^s : \text{core} \\ & + \delta \mathbf{L}^T R_k^s : \text{output}. \end{aligned}$$

If any of the filter stages, input, core, or output can be considered linear or is missing, then the corresponding terms in the above equations must be removed.

### *B. Transconductors With Third-Order Nonlinearity, Zero Offset, and Infinite Output Impedance*

Fully balanced transconductors exhibit (essentially only) odd nonlinearity; moreover, the fifth-order and higher order nonlinear terms are typically negligible compared with the third-order one. Their input offset voltage is usually small, and their output parasitic impedance can be ignored in many cases, typically when the cascode output stage is used.

Under these assumptions, the harmonic distortion of the $G_m\!-\!C$ filter can be derived using the theoretical development in [30]. This subsection compares the reduced form of the more general algorithm introduced here with the one discussed in [30]. The two algorithms have been derived using different structural decomposition of the filters (see the discussion in Section III).

Given the above assumptions, (1) becomes $i = gu + g_3 u^3$, and $\delta$ is given by

$$\delta = \left|\frac{g_3}{g}\right| u_M^2. \tag{58}$$

Moreover, we set $f(u) = p_3 u^3$ where $p_3 = g_3/(\delta g)$.

Following the steps in the previous subsection, we get

$$R_3^c = \frac{1}{4} p_3 \boldsymbol{\eta}_1^c \bullet \left(-3(\boldsymbol{\eta}_1^s)^{\bullet 2} + (\boldsymbol{\eta}_1^c)^{\bullet 2}\right)$$
$$R_3^s = \frac{1}{4} p_3 \boldsymbol{\eta}_1^s \bullet \left(3(\boldsymbol{\eta}_1^c)^{\bullet 2} - (\boldsymbol{\eta}_1^s)^{\bullet 2}\right)$$

and

$$Q_3^s = -\frac{1}{4} p_3 a^3 \mathbf{B}$$

with all other $R_k^c, R_k^s, Q_k^c$, and $Q_k^s$ being zero. Therefore, the algorithm provides the amplitude of the third harmonic.

Since $\mathbf{A} = \mathbf{M}$ and using the above results, we get

$$\boldsymbol{\theta}_3^c = \mathbf{H}_3 \mathbf{A} \left(\mathbf{A} R_3^c + 3\omega R_3^s\right) \tag{59}$$
$$\boldsymbol{\theta}_3^s = \mathbf{H}_3 \mathbf{A} \left(-3\omega R_3^c + \mathbf{A} R_3^s\right) \tag{60}$$

with the remainder of $\boldsymbol{\theta}_k^c$ and $\boldsymbol{\theta}_k^s$ being zero. Similarly, $y_k^c = y_k^s = 0$ for all $k \neq 3, k \geq 2$. Finally, we have

$$\begin{aligned} y_3^c =\, & \frac{3}{4} a^3 \delta p_3 \mathbf{L}^T (9\omega^2 \mathbf{I} + \mathbf{M}^2)^{-1} \omega \mathbf{B} : \text{input} \\ & - \delta \mathbf{L}^T (9\omega^2 \mathbf{I} + \mathbf{M}^2)^{-1} \mathbf{M} \left(\mathbf{M} R_3^c + 3\omega R_3^s\right) : \text{core} \\ & + \delta \mathbf{L}^T R_3^c : \text{output} \\ y_3^s =\, & \frac{1}{4} a^3 \delta p_3 \mathbf{L}^T (9\omega^2 \mathbf{I} + \mathbf{M}^2)^{-1} \mathbf{M} \mathbf{B} : \text{input} \\ & - \delta \mathbf{L}^T (9\omega^2 \mathbf{I} + \mathbf{M}^2)^{-1} \mathbf{M} \left(\mathbf{M} R_3^s - 3\omega R_3^c\right) : \text{core} \\ & + \delta \mathbf{L}^T R_3^s : \text{output}. \end{aligned}$$

We conclude that, in the case of transconductors with third-order nonlinearity, zero offset, and infinite output impedance, the result above is identical to the derivation in [30].

## VI. Extension: Transconductors With Nonidentical Distortion Behaviors

In the case of $G_m\!-\!C$ filters with transconductors having nonidentical nonlinearity, the estimation of the harmonic distortion is more involved; however, it can be done using the steps presented in Sections II–IV.

### *A. System Equations and Definitions*

Consider the $(i, j)$ transconductor in the core of the filter with gain $g_{i,j}$, offset voltage $u_{i,j}^{\text{of}}$, and nonlinearity function $f_{i,j}$ defined as in Section II. To simplify the algebra, we can choose the same value of parameter $\delta$ for all transconductors (e.g., the maximum among all $\delta$). Parameters $\mu_{i,j}$ for the output impedances are defined as before. Therefore, the currents of the core transconductors are

$$i_{i,j} = -g_{i,j} u_{i,j}^{\text{of}} + g_{i,j} v_j + \delta g_{i,j} f_{i,j}(v_j) \tag{61}$$

and the currents of the input transconductors are

$$i_i = -g_i u_i^{\text{of},I} + g_i u + \delta g_i f_i^I(u) \tag{62}$$

where $\mu_i$ and $f_i^I$ are defined accordingly, therefore

$$\begin{aligned} C_i v_i =& \sum_{j=1}^{n} g_{i,j} \left(-u_{i,j}^{\text{of}} + v_j + \delta f_{i,j}(v_j) - \mu_{i,j} v_j\right) \\ & + g_i^I \left(-u_i^{\text{of},I} + u + \delta f_i^I(u) - \mu_i^I v_i\right). \end{aligned} \tag{63}$$

Now, let $\mathbf{U}_{\text{of}} = [u_{i,j}^{\text{of}}]_{i,j=1}^n$ be the filter's core offset matrix, let $\mathbf{U}_{\text{of}}^I = [u_i^{\text{of},I}]_{i=1}^n$ be the input offset matrix, and $\mathcal{M} = [\mu_{i,j}]_{i,j=1}^n, \mathcal{M}^I = [\mu_{i,j}^I]_{i=1}^n, \mathcal{F}(\mathbf{v}) = [f_{i,j}(v_j)]_{i,j=1}^n, \mathcal{F}^I(u) =$

$[f_i^I(u)]_{i=1}^n$ and $\mathbf{G}, \mathbf{G}^I$ are the transconductance matrices defined as before. Then, (63) becomes

$$\begin{aligned}\mathbf{C}\dot{\mathbf{v}} =& -(\mathbf{G} \bullet \mathbf{U}_{\text{of}})\mathbf{1} + \mathbf{G}\mathbf{v} + \delta(\mathbf{G} \bullet \mathcal{F}(\mathbf{v}))\mathbf{1} - (\mathbf{G} \bullet \mathcal{M})\mathbf{v} \\ & - \mathbf{G}^I \bullet \mathbf{U}_{\text{of}}^I + \mathbf{G}^I u + \delta \mathbf{G}^I \bullet \mathcal{F}^I(u) - \text{diag}(\mathbf{G}^I \bullet \mathcal{M}^I)\mathbf{v}\end{aligned}$$

where "$\bullet$" is the Hadamard product. Matrices $\mathbf{M} = \mathbf{C}^{-1}\mathbf{G}$ and $\mathbf{B} = \mathbf{C}^{-1}\mathbf{G}^I$ are defined as before, and

$$\mathbf{A} = \mathbf{G} - \mathbf{G} \bullet \mathcal{M} - \text{diag}(\mathbf{G}^I \bullet \mathcal{M}^I) \tag{64}$$

$$\mathbf{z} = (\mathbf{G} \bullet \mathbf{U}_{\text{of}})\mathbf{1} + \mathbf{G}^I \bullet \mathbf{U}_{\text{of}}^I. \tag{65}$$

System equations for the input and core become

$$\dot{\mathbf{v}} = -\mathbf{z} + \mathbf{A}\mathbf{v} + \delta(\mathbf{G} \bullet \mathcal{F}(\mathbf{v}))\mathbf{1} + \mathbf{G}^I u + \delta \mathbf{G}^I \bullet \mathcal{F}^I(u). \tag{66}$$

The output transconductors (if they exist) give

$$y = \sum_{i=1}^n \left( -g_i^o u_i^{of,O} + g_i^o v_i + \delta g_i^o f_i^o(v_i) \right) \tag{67}$$

$$= -y_{\text{of}} + \mathbf{L}^T \mathbf{v} + \delta \mathbf{L}^T \mathcal{F}^O(\mathbf{v}) \tag{68}$$

where $\mathbf{L}$ is defined as before and $\mathcal{F}^O(\mathbf{v}) = [f_i^O(v_i)]_{i=1}^n$ is the output transconductors' nonlinear functions matrix.

### *B. General Distortion Estimation Algorithm*

We use the (scalar) functions $f_{i,j}, f_i^I$, and $f_i^O$ to derive the functions $f_{i,j,k}^c, f_{i,j,k}^s, f_{i,k}^{I,c}, f_{i,k}^{I,s}, f_{i,k}^{O,c}$, and $f_{i,k}^{O,s}$ based on Definition 4.2. Then, we define the matrix functions $\mathcal{F}_k^c(\mathbf{a},\mathbf{b},\mathbf{c}) = [f_{i,j,k}^c(a_j,b_j,c_j)]_{i,j=1}^n$ and $\mathcal{F}_k^s(\mathbf{a},\mathbf{b},\mathbf{c}) = [f_{i,j,k}^s(a_j,b_j,c_j)]_{i,j=1}^n$, where $\mathbf{a}, \mathbf{b}$, and $\mathbf{c}$ are $n \times 1$ vectors, as well as the vector functions $\mathcal{F}_k^{I,c}(a,b,c) = [f_{i,k}^{I,c}(a,b,c)]_{i=1}^n$ and $\mathcal{F}_k^{I,s}(a,b,c) = [f_{i,k}^{I,s}(a,b,c)]_{i=1}^n$ for the scalars $a, b$ and $c$. We also set $\mathcal{F}_k^{O,c}(\mathbf{a},\mathbf{b},\mathbf{c}) = [f_{i,k}^{O,c}(\mathbf{a},\mathbf{b},\mathbf{c})]_{i=1}^n$ and $\mathcal{F}_k^{O,s}(\mathbf{a},\mathbf{b},\mathbf{c}) = [f_{i,k}^{O,s}(\mathbf{a},\mathbf{b},\mathbf{c})]_{i=1}^n$.

Based on the above, the algorithm in Section IV-D for deriving the harmonic-distortion components and THD of the $G_m - C$ filter is modified as follows. Vectors $\boldsymbol{\eta}_0^c, \boldsymbol{\eta}_1^c$,, and $\boldsymbol{\eta}_1^s$ are given by (41)–(43), respectively, and matrix $\mathbf{H}_k$ is given by (44); parameters $R_k^c, R_k^s, Q_k^c$ and $Q_k^s$ are replaced by $\mathcal{R}_k^c, \mathcal{R}_k^s, \mathcal{Q}_k^c$ and $\mathcal{Q}_k^s$, respectively, and parameters $\mathcal{T}_k^c$ and $\mathcal{T}_k^s$ are introduced as

$$\begin{aligned}\mathcal{R}_k^c &\triangleq \mathbf{M} \bullet \mathcal{F}_k^c(\boldsymbol{\eta}_0^c, \boldsymbol{\eta}_1^c, \boldsymbol{\eta}_1^s) \\ \mathcal{R}_k^s &\triangleq \mathbf{M} \bullet \mathcal{F}_k^s(\boldsymbol{\eta}_0^c, \boldsymbol{\eta}_1^c, \boldsymbol{\eta}_1^s) \\ \mathcal{Q}_k^c &= \mathbf{B} \bullet \mathcal{F}_k^{I,c}(0,0,a) \\ \mathcal{Q}_k^s &= \mathbf{B} \bullet \mathcal{F}_k^{I,s}(0,0,a) \\ \mathcal{T}_k^c &= \mathcal{F}_k^{O,c}(\boldsymbol{\eta}_0^c, \boldsymbol{\eta}_1^c, \boldsymbol{\eta}_1^s) \\ \mathcal{T}_k^s &= \mathcal{F}_k^{O,s}(\boldsymbol{\eta}_0^c, \boldsymbol{\eta}_1^c, \boldsymbol{\eta}_1^s)\end{aligned}$$

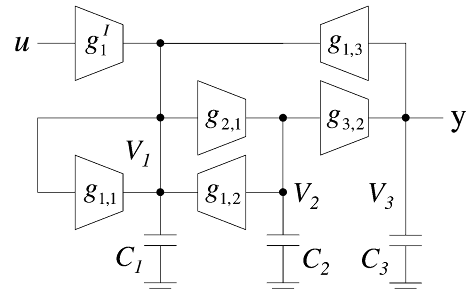


Fig. 8. Third-order Chebyshev type-I low-pass $G_m - C$ filter.

$$\begin{aligned}\boldsymbol{\theta}_k^c &= \mathbf{H}_k \left( \mathbf{A}\mathcal{R}_k^c + k\omega \mathcal{R}_k^s \right) \\ \boldsymbol{\theta}_k^s &= \mathbf{H}_k \left( -k\omega \mathcal{R}_k^c + \mathbf{A}\mathcal{R}_k^s \right) \\ y_k^c &\approxeq \delta \mathbf{L}^T \mathbf{H}_k \left( \mathbf{A}\mathcal{Q}_k^c + k\omega \mathcal{Q}_k^s \right) : \text{input} \\ &\quad + \delta \mathbf{L}^T \boldsymbol{\theta}_k^c : \text{core} \\ &\quad + \delta \mathbf{L}^T \mathcal{T}_k^c : \text{output} \\ y_k^s &\approxeq \delta \mathbf{L}^T \mathbf{H}_k \left( -k\omega \mathcal{Q}_k^c + \mathbf{A}\mathcal{Q}_k^s \right) : \text{input} \\ &\quad + \delta \mathbf{L}^T \boldsymbol{\theta}_k^s : \text{core} \\ &\quad + \delta \mathbf{L}^T \mathcal{T}_k^s : \text{output.}\end{aligned}$$

Finally, $y_1^c, y_1^s, \bar{y}$, and THD are given by (50), (51), (54), and (55), respectively.

## VII. Simulation

Fig. 8 shows the topology of a third-order filter designed in CADENCE on a 0.5-$\mu$ SiGe technology to verify the proposed harmonic-distortion estimation algorithm.

It is a low-pass Chebyshev type-I filter with 2-dB ripple in the pass-band and cutoff frequency $f_{\text{cut}} = 1$ MHz. The filter has no output stage. The prototype transfer function is

$$H^*(s) = \frac{0.327}{s^3 + 0.738s^2 + 1.02s + 0.327} \tag{69}$$

and the state-space matrices used are given by

$$\mathbf{M} = \begin{bmatrix} -4.636 & -6.423 & -2.054 \\ 6.283 & 0 & 0 \\ 0 & 6.283 & 0 \end{bmatrix} \times 10^6 \tag{70}$$

$$\mathbf{B} = \begin{bmatrix} 2.054 \\ 0 \\ 0 \end{bmatrix} \times 10^6$$

$$\mathbf{L} = \begin{bmatrix} 0 \\ 0 \\ 1 \end{bmatrix}. \tag{71}$$

The values of the capacitors are $C_1 = 9$ pF, $C_2 = 8$ pF, and $C_3 = 8$ pF. The gains of the transconductors are $g_{1,1} = -41.7$ $\mu$A/V, $g_{1,2} = -57.8$ $\mu$A/V, $g_{1,3} = -18.5$ $\mu$A/V, $g_{2,1} = 50.3$ $\mu$A/V, $g_{3,2} = 50.3$ $\mu$A/V, and $g_1^I = 18.5$ $\mu$A/V. A prototype of the transconductor was designed using the basic

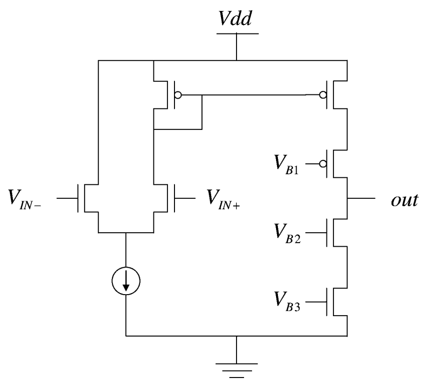


Fig. 9. Transconductor's topology used in the Chebyshev filter.

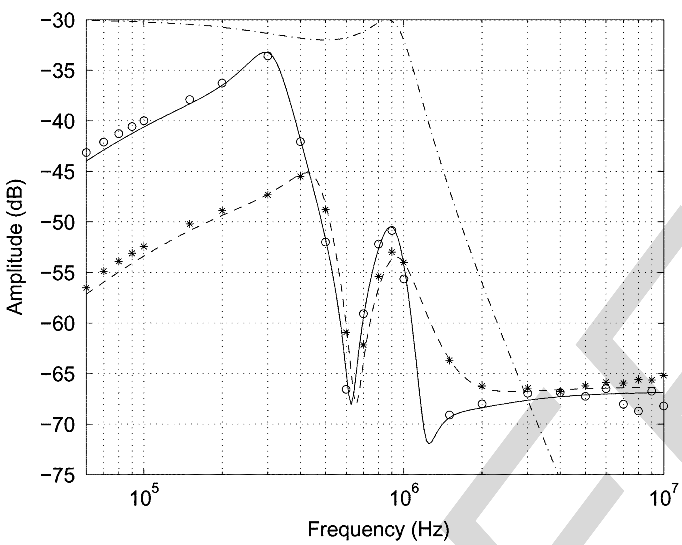


Fig. 10. Simulation results of the low-pass Chebyshev filter in Fig. 8. The dashed–dotted line is the amplitude frequency response shifted by $-30$ dB. The dashed line is the second-harmonic distortion derived using the algorithm. The stars "*" correspond to CADENCE results. The solid line is the third-harmonic distortion derived using the algorithm. The circles "o" correspond to CADENCE results. Input amplitude of 0.5 V has been used in all estimations. The values of the harmonics are normalized with respect to the amplitude of the fundamental.

topology in Fig. 9; then, by uniformly adjusting the widths and biasing currents, the desirable gains were achieved.

CADENCE simulation (dc sweep) was used to extract the $I$–$V$ characteristics of the transconductors. The data was exported to MATLAB to perform polynomial curve fitting.

CADENCE simulation has also been used to extract the harmonic-distortion components at the output of the filter. To this end, transient simulation was done for every frequency point, and the resulting waveform was fed to the fast Fourier transform (FFT) function of SPICE.

The amplitudes of the harmonic-distortion components derived using CADENCE simulation and those derived using the distortion estimation algorithm, implemented in MATLAB, are shown in Fig. 10.

The simulation and theoretical results are in good agreement. The error is within a few decibels, and it is insignificant within the passband.

## VIII. Conclusion

A fast one-pass harmonic-distortion estimation algorithm for $G_m\!-\!C$ filters has been introduced. It is based on state-space representation of the filter and applies directly to $G_m\!-\!C$ filters of any order with weakly nonlinear MOS transconductors exhibiting any type of nonlinearity. It is formed out of a small set of simple explicit formulas, involving the filter's structural matrices, that can be easily implemented in MATLAB.

The results of the algorithm have been compared with CADENCE simulation in the case of the a single-ended $G_m\!-\!C$ filter with weakly nonlinear transconductors designed on a 0.5-$\mu$ m technology. The results of the algorithm and CADENCE simulation were found in good agreement.

## Appendix I
## Solution of the Linear System

The complete solution of the dynamical system

$$\dot{\mathbf{x}}(t) = \mathbf{A}\,\mathbf{x}(t) + \boldsymbol{\beta}\cos(wt) + \boldsymbol{\gamma}\sin(wt) \tag{72}$$

can be found in [32]

$$\begin{aligned}\mathbf{x}(t) &= e^{\mathbf{A}t}\mathbf{x}(0) + \int_0^t e^{\mathbf{A}(t-\tau)}(\boldsymbol{\gamma}\sin(w\tau) + \boldsymbol{\beta}\cos(w\tau))d\tau \\ &= -(\mathbf{A}^2 + w^2\mathbf{I})^{-1}(\mathbf{I}w\cos(wt) + \mathbf{A}\sin(wt) - we^{\mathbf{A}t})\boldsymbol{\gamma} \\ &\quad - (\mathbf{A}^2 + w^2\mathbf{I})^{-1}\left(\mathbf{A}\cos(wt) - \mathbf{I}w\sin(wt) - \mathbf{A}e^{\mathbf{A}t}\right)\boldsymbol{\beta} \\ &\quad + e^{\mathbf{A}t}\mathbf{x}(0).\end{aligned}$$

By assumption, the dynamical system is asymptotically stable (i.e., matrix $\mathbf{A}$ is Hurwitz) so $\lim_{t\to\infty} \| e^{\mathbf{A}t} \|_2 = 0$ and the steady-state part of the system's solution is

$$\begin{aligned}\mathbf{x}_{ss}(t) = &-(w^2\mathbf{I} + \mathbf{A}^2)^{-1}(\mathbf{A}\boldsymbol{\gamma} - w\boldsymbol{\beta})\sin(wt) \\ &- (w^2\mathbf{I} + \mathbf{A}^2)^{-1}(\mathbf{A}\boldsymbol{\beta} + w\boldsymbol{\gamma})\cos(wt).\end{aligned} \tag{73}$$

## References

[1] Y. Tsividis and J. O. Voorman, *Integrated Continuous-Time Filters*. New York: IEEE Press, 1993.
[2] Y. Tsividis, "Intergrated continuous-time filter design—An overview," *IEEE J. Solid-State Circuits*, vol. 29, no. 3, pp. 166–176, Mar. 1994.
[3] S. Willingham and K. Martin, *Integrated Video-Frequency Continuous-Time Filters*. Norwell, MA: Kluwer, 1995.
[4] R. L. Geiger and E. Sanchez-Sinencio, "Active filter design using operational transconductance amplifiers: A tutorial," *IEEE Circuits Devices Mag.*, vol. 1, no. 2, pp. 20–32, Mar. 1985.
[5] J. E. Franca and Y. Tsividis, Eds., *Design of Analog-Digital VLSI Circuits for Telecommunications and Signal Processing*, 2nd ed. Englewood Cliffs, NJ: Prentice-Hall, 1994.
[6] V. Gopinathan, Y. Tsividis, K. Tan, and R. Hester, "Design considerations for high-frequency continuous-time filters and implementation of an anti-aliasing filter for digital video," *IEEE J. Solid-State Circuits*, vol. 25, no. 6, pp. 1368–1378, Dec. 1990.
[7] J. M. Khoury, "Design of a 15-MHz CMOS continuous-time filter with on-chip tuning," *IEEE J. Solid-State Circuits*, vol. 26, no. 12, pp. 1988–1997, Dec. 1991.
[8] J. Silva-Martinez, M. Steyaert, and W. Sansen, "A 10.7 MHz 68-db SNR CMOS continuous-time filter with on-chip automatic tuning," *IEEE J. Solid-State Circuits*, vol. 27, no. 12, pp. 1843–1853, Dec. 1992.

[9] W. M. Snelgrove and A. Shoval, “A balanced 0.9 $\mu$m CMOS transconductance-C filter tunable over the VHDF range,” *IEEE J. Solid-State Circuits*, vol. 27, no. 5, pp. 314–323, Mar. 1992.

[10] C.-C. Hung, K. Halonen, M. Ismail, V. Porra, and A. Hyogo, “A low-voltage, low-power CMOS fifth-order elliptic $G_m$-C filter for baseband mobile, wireless communication,” *IEEE Trans. Circuits Syst. Video Technol.*, vol. 7, no. 4, pp. 584–593, Aug. 1997.

[11] H. Voorman and H. Veenstra, “Tunable high-frequency $G_m$-c filters,” *IEEE J. Solid-State Circuits*, vol. 35, no. 8, pp. 1097–1108, Aug. 2000.

[12] J.-Y. Lee, C.-C. Tu, and W.-H. Chen, “A 3 V linear input range tunable CMOS transconductor and its applications to a 3.3 V 1.1 MHz Chebyshev low-pass $G_m$-c filter for ADSL,” in *Proc. IEEE Custom Integr. Circuits Conf.*, 2000***[Author: Please provide page numbers.--Ed.]***.

[13] D. A. Johns and K. Martin, *Analog Integrated Circuit Design*. New York: Wiley, 1997.

[14] Y. Tsividis, N. Krishnapura, Y. Palaskas, and L. Toth, “Internally varying analog circuits minimize power dissipation,” *IEEE Circuits Devices Mag.*, vol. 19, no. 1, pp. 63–72, Mar. 2003.

[15] Z. Y. Chang, D. Haspeslagh, J. Boxho, and D. Macq, “A highly linear CMOS $G_m$-c bandpass filter for video applications,” in *Proc. IEEE Custom Integr. Circuits Conf.*, 1996***[Author: Please provide page numbers.--Ed.]***.

[16] Y. Tsividis, M. Banu, and J. Khoury, “Continuous-time MOSFET-C filters in VLSI,” *IEEE J. Solid-State Circuits*, vol. SSC-21, no. 1, pp. 15–30, Feb. 1986.

[17] Y. Tsividis, Z. Czarnul, and S. C. Fang, “MOS transconductors and intergrators with high linearity,” *Electron. Lett.*, vol. 22, pp. 245–246, Feb. 1986.

[18] F. Krummenacher and N. Johl, “A 4-MHz CMOS continuous-time filter with on-chip automatic tuning,” *IEEE J. Solid-State Circuits*, vol. 23, no. 3, pp. 750–758, Jun. 1988.

[19] F. Yuan and A. Opal, “Distortion analysis of periodically switched nonlinear circuits using time-varying Volterra series,” *IEEE Trans. Circuits Syst. I, Fundam. Theory Appl.*, vol. 48, no. 6, pp. 726–738, Jun. 2001.

[20] J. A. Cherry and W. M. Snelgrove, “On the characterization and reduction of distortion in bandpass filters,” *IEEE Trans. Circuits Syst. I, Fundam. Theory Appl.*, vol. 45, no. 5, pp. 523–537, May 1998.

[21] P. Wambacq, G. Gielen, P. Kinget, and W. Sansen, “High-frequency distortion analysis of analog integrated circuits,” *IEEE Trans. Circuits Syst. II, Analog Digit. Signal Process.*, vol. 46, no. 3, pp. 335–344, Mar. 1999.

[22] G. Palumbo and S. Pennisi, “High-frequency harmonic distortion in feedback amplifiers: Analysis and applications,” *IEEE Trans. Circuits Syst. I, Fundam. Theory Appl.*, vol. 50, no. 3, pp. 328–340, Mar. 2003.

[23] S. Cannizzaro, G. Palumbo, and S. Pennisi, “Accurate estimation of high-frequency harmonic distortion in two-stage Miller OTAs,” *IEE Proc. Circuits, Devices Syst.*, vol. 152, no. 5, pp. 417–424, Oct. 2005.

[24] ——, “Effects of nonlinear feedback in the frequency domain,” *IEEE Trans. Circuits Syst. I, Reg. Papers*, vol. 53, no. 2, pp. 225–234, Feb. 2006.

[25] Y. Palaskas and Y. Tsividis, “Dynamic range optimization of weakly nonlinear, fully balanced, $G_m$-C filters with power dissipation constraints,” *IEEE Trans. Circuits Syst. II, Analog Digit. Signal Process.*, vol. 50, no. 10, pp. 714–727, Oct. 2003.

[26] E. A. Coddington and N. Levinson, *Theory of Ordinary Differential Equations*. New York: McGraw-Hill, 1955.

[27] T. Kato, *Perturbation Theory for Linear Operators*. New York: Springer-Verlag, 1985.

[28] J. Simmonds and J. Mann, Jr., *A First Look at Perturbation Theory*, 2nd ed. New York: Dover, 1997.

[29] H. Khalil, *Nonlinear Systems*, 3rd ed. Upper Saddle River, NJ: Prentice Hall, 2002.

[30] Z. Zhang, A. Celik, and P. Sotiriadis, “State space harmonic distortion modeling in weakly nonlinear, fully balanced Gm-C filters—A modular approach resulting in closed form,” *IEEE Trans. Circuits Syst. I, Reg. Papers*, vol. 53, no. 1, pp. 48–59, Jan. 2006.

[31] A. Celik, Z. Zhang, and P. Sotiriadis, “A state-space approach to intermodulation distortion estimation in fully balanced bandpass $G_m-C$ filters with weak nonlinearities,” *IEEE Trans. Circuits Syst. I, Reg. Papers*, to be published***[Author: Please update the status of this paper.--Ed.]***.

[32] T. Kailath, *Linear Systems*. Englewood Cliffs, NJ: Prentice-Hall, 1980.

**Paul P. Sotiriadis** (M’XX) **[AUTHOR: PLEASE PROVIDE YOUR YEAR OF MEMBERSHIP.—ED.]** received the diploma in electrical engineering and computer science from the **[AUTHOR: PLEASE PROVIDE THE YEARS THE UNDERGRADUATE AND GRADUATE DEGREES WERE RECEIVED.—ED.]** National Technical University of Athens (NTUA), Athens, Greece, the M.S. degree in electrical engineering from Stanford University, Stanford, CA, and the Ph.D. degree in electrical engineering and computer science from the Massachusetts Institute of Technology, Cambirdge, in 2002.

Since June 2002, he has been an Assistant Professor with the Department of Electrical and Computer Engineering, The Johns Hopkins University, Baltimore, MD. His research interests include design, optimization, and mathematical modeling of analog and mixed-signal circuits, RF and microwave circuits, fine frequency synthesis, and interconnect networks in deep-sub-micron technologies. He serves as an Associate Editor of the IEEE TRANSACTIONS ON CIRCUITS AND SYSTEMS II—EXPRESS BRIEFS.

**Abdullah Çelik** (S’XX) **[AUTHOR: PLEASE PROVIDE YOUR YEAR OF MEMBERSHIP.—ED.]**received the B.S., degree in electrical and electronics engineering from the Bilkent University, Ankara, Turkey, in 2002, and the M.S.E. degree from The Johns Hopkins University, Baltimore, MD, in 2004.

He is currently a Research Assistant with the Adaptive Microsystems Laboratory, The Johns Hopkins University. His research interests include the ultralow-power design and implementation of custom VLSI systems for acoustical sensors, analog signal processing circuits, and MEMs structures for audio reception.

**Dimitrios Loizos** (S’XX) **[AUTHOR: PLEASE PROVIDE YOUR YEAR OF MEMBERSHIP.—ED.]** received the diploma in electrical and computer engineering from the National Technical University of Athens (NTUA), Athens, Greece, in 2003, and the M.S.E. degree in electrical and computer engineering from The Johns Hopkins University, Baltimore, MD, in 2005.

He is currently a Research Assistant with the RF and Microwaves Laboratory, The Johns Hopkins University. His current research interests include model-free optimization techniques and their VLSI implementation, RF and microwave circuits, as well as MMIC design.

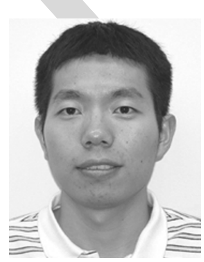

**Zhaonian Zhang** (S’XX) **[AUTHOR: PLEASE PROVIDE YOUR YEAR OF MEMBERSHIP.—ED.]** received the B.S.E. degree in electronic engineering from the Beijing Institute of Technology, Beijing, China, in 2001, and the M.S.E. degree in electrical and computer engineering from The Johns Hopkins University, Baltimore, MD, in 2004.

He is currently a Research Assistant with the Sensory Communications and Microsystems Lab, The Johns Hopkins University. His current research interests include ultra-wideband systems, MEMS structures for acoustic systems, and digital system design.

Mr. Zhang is a member of Tau Beta Pi.